# CT in the evaluation of the orbit and the bony interorbital distance.

M F Mafee, S Pruzansky, M M Corrales, M G Phatak, G E Valvassori, G D Dobben and V Capek

*AJNR Am J Neuroradiol* 1986, 7 (2) 265-269
http://www.ajnr.org/content/7/2/265

# CT in the Evaluation of the Orbit and the Bony Interorbital Distance

Mahmood F. Mafee[1]
Samuel Pruzansky*,[2]
Manuel M. Corrales[1]
Mohan G. Phatak[1]
Galdino E. Valvassori[1]
Glen D Dobben[1]
Vlastimil Capek[1]

**The distance between the orbits and their individual dimensions are important in the diagnosis of craniofacial anomalies. Most observers rely on standard radiographs for measuring the bony interorbital distance. Tomography of the skull base and orbital computed tomography (CT) can also be used. This article describes the normal range of the bony interorbital distance and other useful orbital linear and angular measurements as determined from a series of CT scans of the orbits in 400 adults who had CT for other purposes. The normal interorbital distance measured at the posterior border of the frontal processes of the maxilla on nonrotated scans, in the plane of the optic nerve, ranges from 2.29 to 3.21 cm (average, 2.67 cm) in men and 2.29 to 3.20 cm (average, 2.56 cm) in women. The widest interorbital distance lies behind the posterior poles of the globes. This ranges from 3.16 to 4.10 cm (average, 3.37 cm) in men and 2.93 to 3.67 cm (average, 3.20 cm) in women.**

The eyes are often involved in craniofacial malformations, which includes orbital clefts and orbital hypotelorism and hypertelorism. Measurement of the bony interorbital distance is useful in establishing the severity of the hypertelorism. Surgical treatment of hypertelorism involves translocation of the globes toward the midline by lateral wall osteotomy at a point posterior to the equator of the eye [1]. The degree of hypertelorism and character of the lateral orbital wall determine the type of lateral wall osteotomy [1]. Computed tomography (CT) is very helpful in preoperative evaluation of such patients. The CT scan may also show an encephalocele or a porencephalic cyst as an additional feature of the malformation [2]. This is a report of measurements of the normal orbit with reference to hypertelorism and other anomalies.

## Materials and Methods

Four hundred adults (200 men aged 18–82, average age 52; 200 females aged 17–88, average age 54) were examined with the General Electric CT 7800 scanner (+500 to −500 scale). To obtain uniform images for linear measurements, the window width and level were set at 250 and 50, respectively, for all cases. Data were collected from patients with normal orbits who were studied for suspicion of brain infarction, hearing loss, and brain tumors. None had any underlying craniofacial anomaly or congenital malformations. The patients were Caucasian except for a few who were Oriental.

In all instances 5 or 10 mm sections were obtained parallel to the infraorbital-meatal plane. The optic nerve and canal are roughly parallel to this plane. For this study, data were collected only from the nonrotated axial sections in the plane of the optic nerves (fig. 1A).

The horizontal CT sections through the orbits at this level generally show two patterns: (1) a parallel separation of the medial orbital walls and (2) a fusiform or lateral spread of the ethmoidal air cells with the widest separation of the orbital walls occurring posterior to the posterior pole of the globe. The distance between the medial walls of the bony orbits at various points and other linear and angular measurements are illustrated in figures 1 and 2. Several reference points have been used. *Anterior pole* is applied to the central point of the anterior curvature of the eyeball and *posterior pole* to the central point of its posterior

Received April 1, 1981; accepted after revision August 9, 1985.

Presented at the annual meeting of the American Roentgen Ray Society, San Francisco, March 1981.

* Deceased.

[1] Department of Diagnostic Radiology, University of Illinois Hospital, Chicago, IL 60612. Address reprint requests to M. F. Mafee, Department of Radiology, Eye and Ear Infirmary, 1855 W. Taylor St., Chicago, IL 60612.

[2] Center for Craniofacial Anomalies, University of Illinois Hospital, Chicago, IL 60612.

***AJNR* 7:265–269, March/April 1986**
0195–6108/86/0702–0265

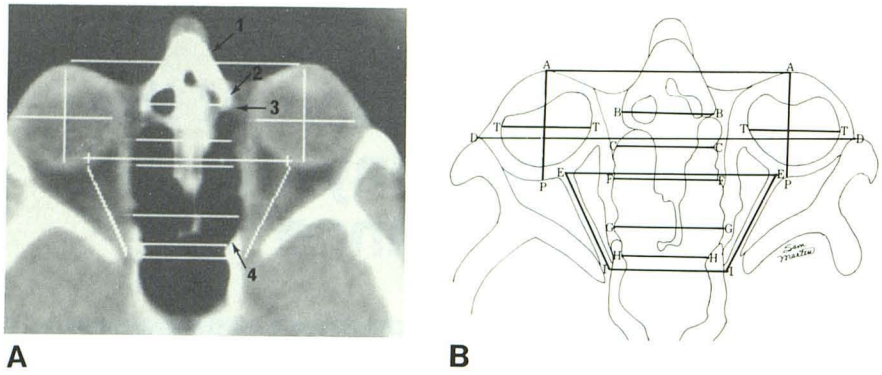


Fig. 1.—**A**, Axial CT scan of orbits at level of plane of optic nerves shows outline of globes, lenses, vitreous bodies, level of medial check ligaments (3), medial and lateral rectus muscles, optic nerves, and retroorbital fat compartments. Note nasal bone (1) and frontal process of maxilla (2) on each side. Frontal process of maxilla forms most anterior part of medial wall of bony orbit. Lacrimal bone is seen as a thin, increased density immediately posterior to frontal process of maxilla. Lamina papyracea is seen as very thin density hardly distinguishable from medial aspect of medial rectus. Posterior to that is most posterior part of medial wall of bony orbit (4), which is related to anterior part of sphenoid sinus. (Reprinted from [3].) **B**, Diagram showing different points selected for various measurements presented in table 1.

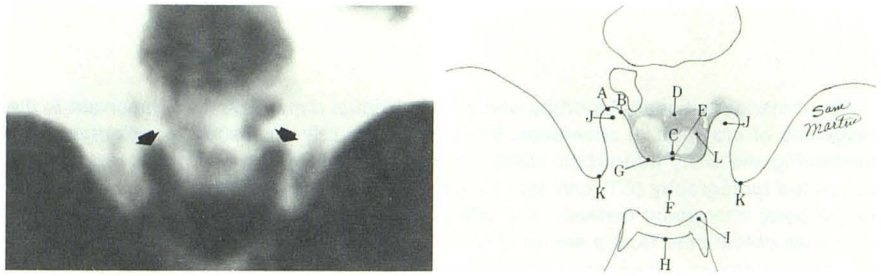


Fig. 2.—**A**, Axial CT scan of head at level of planum sphenoidale and anterior roots of lesser wings of sphenoid shows cranial openings (*arrows*) of optic canals. **B**, Diagram showing structures in **A**. A = cranial opening of optic canal; B = anterior root of lesser wing of sphenoid; C = posterior border of chiasmatic groove; D = planum sphenoidale; E = tuberculum sellae; F = pituitary fossa; G = middle clinoid; H = dorsum sellae; I = posterior clinoid; J = midportion of cranial opening of optic canal; K = anterior clinoid; L = anterior border of chiasmatic groove.

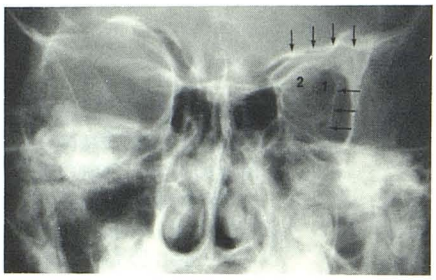


Fig. 3.—10-year-old girl with left microphthalmia. Posteroanterior view of skull. Left orbital plate of frontal bone (*vertical arrows*), left lesser wing of sphenoid (2), and left maxillary sinus are hypoplastic; superior orbital fissures are asymmetric (1). Note difference between oblique lines (*horizontal arrows*), which represent cortices of temporal surface of great wings of sphenoid bone.

curvature. These points are designated as point A and point P, respectively (fig. 1). A line joining the two poles forms the optic axis (AP). The primary axes of the two eyeballs are nearly parallel. The lacrimal bone and the lamina papyracea cast a thin line of increased density posterior to the frontal process of the maxilla. CT is the best method to evaluate the course and angle of the optic nerves. The optic canal can also be demonstrated. The cranial opening of the optic canal is well demonstrated in figure 2A. The optic canal lies between the two roots of the lesser wing and is bounded medially by the body of the sphenoid bone. The anterior root is broad and flat and is continuous with the planum sphenoidale. The posterior root is shorter and thicker and connected to the body of the sphenoid opposite the posterior border of the sulcus chiasmatis.

In figure 2, the JJ line is considered the distance between the central optic canals at their cranial openings. With regard to the globe, the AP distance (fig. 1) is considered the anteroposterior diameter and the TT distance is considered the transverse diameter of the eyeball. For the measurement of the transverse diameter of the globe exclusive of the thickness of the lateral and medial rectus muscles, measurements were obtained with the cursor placed at the junction of the scleral ring and images of the rectus muscle. For the measurement of the eyeball diameters, no attempt was made to correlate the values obtained with possible myopia or hypermetropia.

## Results

Our results (table 1) show that the medial orbital walls, in a horizontal section taken at the plane of the optic nerves, tend to be parallel or divergent (fig. 1A). The narrowest interorbital distance at this section level is at the posterior border of the frontal process of the maxilla (fig. 1), and the widest distance is at or posterior to the posterior poles of the eyeballs. There was a slight difference between the right and left eyeball measurements.

## Discussion

In the diagnosis of craniofacial anomalies, thorough radiographic inspection of the cranial vault, orbits, facial bones, and temporal bones and their interrelationships yields useful diagnostic information [3]. CT is particularly useful in identifying bony and soft-tissue features in these regions.

### *Anatomic and Developmental Considerations*

Under normal conditions the eye directs orbital growth. During the first year of life, the eye practically doubles in volume and attains more than 50% of its adult volume [4]. By the end of the third year, 75% of adult volume is achieved (similar to neural growth [4]). The shape of the orbital cranial junction is also influenced by development of the brain and skull [5]. When the brain is underdeveloped but the eye is normal, the orbital plate of the frontal bone is usually elevated into the anterior fossa of the skull. In microcephaly the orbits

TABLE 1: **CT Orbital Measurements in 400 Adults**

| Line, Description | Measurement (cm) | | | | | |
|---|---|---|---|---|---|---|
| | Minimum | | Maximum | | Mean | |
| | Male | Female | Male | Female | Male | Female |
| AA, Approximates interpupillary distance | 6.26 | 6.21 | 7.51 | 7.50 | 6.78 | 6.63 |
| BB, BIOD measured at posterior border of frontal processes of maxillae | 2.29 | 2.29 | 3.21 | 3.20 | 2.67 | 2.56 |
| CC, BIOD measured posterior or at level of orbital equator (useful orbits) | 2.63 | 2.56 | 3.50 | 3.30 | 2.80 | 2.83 |
| DD, Distance between anterior margin of frontal processes of zygomatic bones at level of plane of optic nerves | 9.18 | 9.29 | 10.13 | 11.00 | 9.73 | 9.97 |
| EE, Distance between optic nerves where they enter eyeballs | 5.16 | 4.78 | 6.40 | 6.00 | 5.43 | 5.27 |
| FF, BIOD measured at level of posterior poles of eyeballs | 2.87 | 2.56 | 3.7 | 3.51 | 3.10 | 2.97 |
| GG, BIOD measured at its widest part (usually posterior to FF line) | 3.16 | 2.93 | 4.10 | 3.67 | 3.37 | 3.20 |
| HH, BIOD measured at its most posterior part (apex of bony orbit) | 2.16 | 2.43 | 3.37 | 3.23 | 2.73 | 2.80 |
| II, Distance between superior orbital fissures at apex of bony orbit | 2.90 | 2.70 | 3.83 | 3.63 | 3.10 | 3.00 |
| JJ, Distance between central portion of cranial opening of optic canals | 2.20 | 2.01 | 2.73 | 2.70 | 2.30 | 2.20 |
| KK, Distance between tips of anterior clinoid processes | 2.31 | 2.43 | 3.21 | 3.16 | 2.80 | 2.83 |
| EI, Length of intraorbital part of optic nerve: | | | | | | |
| Right | 2.70 | 2.40 | 3.80 | 3.23 | 3.10 | 2.90 |
| Left | 2.60 | 2.40 | 3.80 | 3.21 | 3.20 | 2.80 |
| AP, Anteroposterior diameter of eyeball: | | | | | | |
| Right | 2.50 | 2.39 | 2.90 | 2.70 | 2.80 | 2.50 |
| Left | 2.40 | 2.40 | 2.80 | 2.80 | 2.70 | 2.63 |
| TT, Transverse diameter of eyeball: | | | | | | |
| Right | 2.50 | 2.40 | 2.80 | 2.90 | 2.70 | 2.71 |
| Left | 2.50 | 2.50 | 2.90 | 2.90 | 2.80 | 2.83 |
| Angle between optic nerve axes (in degrees) | 35° | 36.5° | 50° | 51.5° | 41° | 42.3° |

Note.—BIOD = bony interorbital distance.

Fig. 4.—In mandibulofacial dysostosis, orbits often show deficiency of lateral orbital floor, representing orbital cleft. In severe malar hypoplasia, lateral orbital wall is formed by greater wing of sphenoid and zygomatic process of frontal bone. (Courtesy of Samuel Pruzansky and Paul Tessier.)

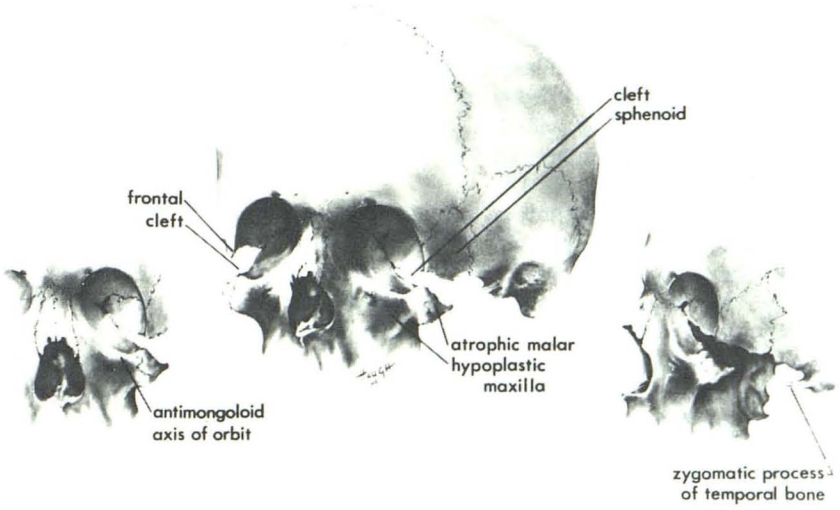


are usually circular and the roofs are highly arched [5]. When the eye is underdeveloped but the brain is normal, the orbital plate of the frontal bone appears hypoplastic and the vertical or calvarial part is usually normal (fig. 3).

In coronal suture synostosis, the orbit on the side of fusion is elongated superiorly and laterally imparting a harlequin appearance (plagiocephaly). Correction of the cranial deformity can lead to spontaneous correction of the orbital deformity in some instances [6].

In mandibulofacial dysostosis the orbits may be defective inferolaterally due to malar bone hypoplasia. With tomography the deficiency of the lateral orbital floor (orbital cleft) can be demonstrated [3]. In cases of severe malar hypoplasia the laterall wall of the orbit is formed by the greater wing of the sphenoid and the zygomatic process of the frontal bone (fig. 4).

The medial wall of the orbital cavity is extremely thin, except in its most posterior portion, where it is related to the anterior

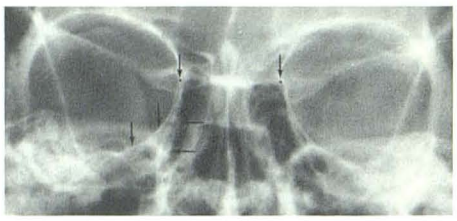

Fig. 5.—Caldwell (inclined posteroanterior) view of skull. Lamina papyracea of ethmoid is demonstrated by two lines on each side. *Horizontal arrows* point to anterior part of lamina papyracea and *lower vertical arrows* point to posterior part of it. *Upper vertical arrows* point to black dots, which indicate points at which usually interorbital distance is measured on radiograph. (Reprinted from [3].)

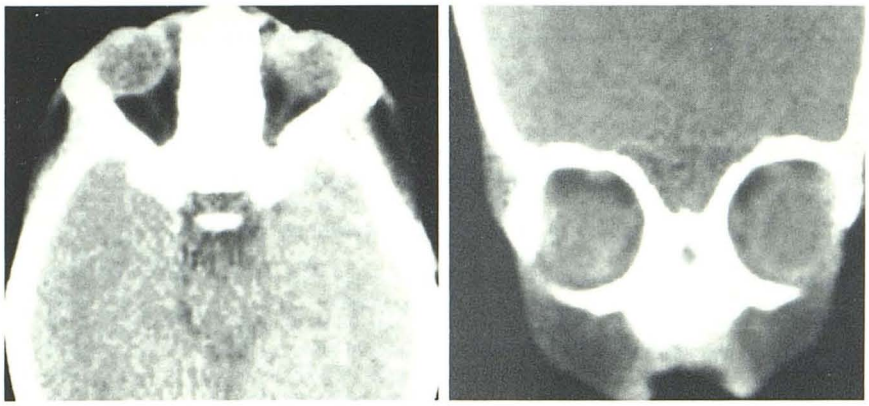

A B

Fig. 6.—4-year-old boy born without a nose and with Left microphthalmus and apparent hypertelorism. **A**, Left globe slightly smaller than right. Increased soft tissue between medial wall of orbit and globe anteriorly has clinical appearance of hypertelorism. In fact, interorbital bony distance is normal. **B**, Coronal view. Irregular, thick compact bone in anterior midface with absent nasal structures and maxillary sinuses.

portion of the sphenoid sinus and forms its lateral wall. This orbital wall slopes gently downward and laterally into the floor. This is best seen on the Caldwell view of the skull (fig. 5), where the anterior and posterior parts of the lamina papyracea are well demonstrated. The lacrimal bones, which are the smallest and the most fragile of the cranial bones, are situated at the front of the medial walls of the orbits. Their anterior border articulates with the frontal process of the maxilla, the posterior border with the orbital plate (lamina papyracea) of the ethmoid (fig. 1A).

The value of CT can be appreciated in a patient with severe nasomaxillary hypoplasia who was found clinically to have hypertelorism (fig. 6). CT clearly shows the nasal and maxillary deformity. The bony interorbital distance is normal. Increased soft tissue in the nasoorbital angles has created the appearance of pseudohypertelorism or telecanthus [7].

The bony interorbital distance is an essential measurement in diagnosing orbital hypotelorism or hypertelorism [8–12]. Before CT the principal methods used for such measurements have been based on conventional posteroanterior projection and cephalometric radiography. While such projections may be useful in the study of normal subjects, their utility in pathologic states is questionable.

One major problem is that a conventional film is a composite of various structures at different planes; in some patients measurement landmarks are difficult to identify. The best methods to evaluate the bony interorbital distance are base tomography and CT. CT also provides significant information on the orbits, ethmoid, sphenoid sinuses, facial bones, the median and paramedian craniofacial cleft, and central nervous system pathology.

The bony interorbital distance was first defined by Cameron [8] in a small number of dried skulls as the maximum distance between the medial walls of the bony orbits measured at the juncture of the crista lacrimalis posterior with the frontolacrimal suture. Currarino and Silverman [9], in their studies of arhinencephaly and trigonocephaly, measured the bony interorbital distance between the medial walls at what was described to be the junction between each medial angular process of the frontal bone with the maxillary and lacrimal bones.

In order to provide a statistically more reliable standard, Gerald and Silverman [10] repeated the original work of Currarino and Silverman [9] using the same technical factors, and studied 100 patients in each year of age from birth to 12 years. Hansman [11] presented measurements of the interorbital distance and thickness of the skull based on radiographs of the skull and paranasal sinuses in a large group of healthy subjects. According to him, from "infancy to adulthood, the bony interorbital distance for girls is consistently narrower than for boys. Starting at 1 year 6 months, there is gradual increase in the size of the measurements for both sexes. At about 13 years of age the girl's growth began to level off. Since the boys continue to increase to the age of about 21 years, the measurements in girls fall more markedly below the boys as growth is completed." The average adult measurement in women is 25 mm and in men 28 mm [11].

CT of the orbit provides along with other information an opportunity to evaluate the distance between the orbits and, if necessary, any other linear or angular measurements. The lacrimal bones and the orbital plates of the ethmoid cast a thin line of increased density on the CT scan and, therefore, the bony interorbital distance can be measured at any desired points. Since orbital hypertelorism and hypotelorism are associated with a variety of other malformations affecting the hard and soft tissues [13], it is essential that appropriate radiographic methods including conventional radiography, cephalometry, tomography, and CT be used. Further study

of more cases to determine the normal standards for the bony interorbital distance in infancy and childhood is needed to determine the patterns of growth. The bony interorbital distance in pathologic conditions and the anatomic factors contributing to reduced orbital capacity and exophthalmos and the effect of form on function in Apert and Crouzon syndromes can be effectively evaluated by CT. This problem is being studied in various craniofacial anomalies and will be taken up in a subsequent publication.

ACKNOWLEDGMENT

We thank Leah M. Freeman for secretarial assistance.

REFERENCES

1. Converse JM, McCarthy JG, Wood-Smith D. Reconstructive plastic surgery for orbital hypertelorism. In: Converse JM, McCarthy JG, Wood-Smith D, eds. *Symposium on diagnosis and treatment of craniofacial anomalies*, vol 20. St. Louis: Mosby, **1979**:207–221.
2. Becker MH. Computed tomography in the evaluation of the craniofacial malformations. In: Converse JM, McCarthy JG, Wood-Smith D, eds. *Symposium on diagnosis and treatment of craniofacial anomalies*, vol 20. St. Louis: Mosby, **1979**:182–185.
3. Mafee MF, Valvassori GE. Radiology of the craniofacial anomalies. *Otolaryngol Clin North Am* **1981**;14:939–988
4. Tessier P. The definitive plastic surgical treatment of the severe facial deformities of craniofacial dysostosis. Crouzon's and Apert's diseases. *Plast Reconstr Surg* **1971**;48:419–442
5. Campbell JA. Craniofacial anomalies. In: Newton TH, Potts DG, eds. *Radiology of the skull and brain*, vol 1, book 2. St. Louis: Mosby, **1971**:571–633
6. Pruzansky S. Time: the fourth dimension in syndrome analysis applied to craniofacial malformations. *Birth Defects* **1977**;13:3–28
7. Mustarde JC. Epicanthus and telecanthus. *Br J Plast Surg* **1963**;16:346–356
8. Cameron J. Interorbital width. New cranial dimension. Its significance in modern and fossil man in lower mammals. *Am J Phys Anthropol* **1931**;15:509–515
9. Currarino G, Silverman FN. Orbital hypotelorism, arhinencephaly, and trigoncephaly. *Radiology* **1960**;74:206–216
10. Gerald BE, Silverman FN. Normal and abnormal interorbital distances with special reference to mongolism. *AJR* **1956**;95:154–161
11. Hansman CF. Growth of interorbital distance and skull thickness as observed in roentgenographic measurements. *Radiology* **1966**;86:87–96
12. Morin J, Hiu J, Anderson J, Grainger R. A study of growth in the interorbital region. *Am J Ophthalmol* **1936**;56:895
13. Tessier P. Orbital hypertelorism. (1) Successful surgical attempts, material and methods, causes and mechanism. *Scand J Plast Reconstr Surg* **1972**;6:155–185